Tunable Fano resonances in transport through microwave billiards

S. Rotter,[1,*] F. Libisch,[1] J. Burgdörfer,[1] U. Kuhl,[2] and H.-J. Stöckmann[2]

[1]*Institute for Theoretical Physics, Vienna University of Technology, A-1040 Vienna, Austria*
[2]*Fachbereich Physik, Philipps-Universität Marburg, D-35032 Marburg, Germany*

We present a tunable microwave scattering device that allows the controlled variation of Fano line shape parameters in transmission through quantum billiards. Transport in this device is nearly fully coherent. By comparison with quantum calculations, employing the modular recursive Green's-function method, the scattering wave function and the degree of residual decoherence can be determined. The parametric variation of Fano line shapes in terms of interacting resonances is analyzed.

Asymmetric Fano line shapes are a ubiquitous feature of resonance scattering when (at least) two different pathways connecting the entrance with the exit channel exist. Fano resonances have been observed in a wide array of different subfields of physics starting with photoabsorption in atoms [1–3], electron and neutron scattering [4,5], Raman scattering [6], photoabsorption in quantum well structures [7], scanning tunnel microscopy [8], and ballistic transport through quantum dots ("artificial atoms") [9–12]. Interest in observing and analyzing Fano profiles is driven by their high sensitivity to the details of the scattering process. For example, since Fano parameters reveal the presence and the nature of different (non) resonant pathways, they can be used to determine the degree of coherence in the scattering device. This is due to the fact that decoherence converts Fano resonances into the more familiar limiting case of a Breit-Wigner resonance. Furthermore, they provide detailed information on the interaction between nearby resonances leading to "avoided crossings" in the complex plane [13,14], and to stabilization of discrete states in the continuum ("resonance trapping" [15,16]).

Exploiting the equivalence of the scalar Helmholtz equation for electromagnetic radiation in cavities with conducting walls and the Schrödinger equation subject to hard-wall boundary conditions [17], we have designed a scattering device (Fig. 1) that allows the controlled tuning of Fano resonances for transport through quantum billiards. The evolution of the Fano parameters as a function of the tuning parameter, in the present case the degree of opening of the leads, can be traced in unprecedented detail, since decoherence due to dissipation is kept at a low level. By comparison with calculations employing the modular recursive Green's function method (MRGM) [11,18], the parametric variation of Fano resonances and the degree of decoherence can be quantitatively accounted for. Furthermore, the relevant pathways can be unambiguously identified in terms of wave functions representing the contributing scattering channels. Due to the equivalence between microwave transport and single-electron motion in two dimensions, our device also simulates ballistic electron scattering through a quantum dot.

In contrast to recent investigations of mesoscopic dots and single-electron transistors [9,12,19], where comparison between theory and experiment has remained on a mostly qualitative level, our model system allows for a detailed quantitative analysis of all features of tunable resonances.

Our microwave scattering device consists of two commercially available waveguides (height $h=7.8$ mm, width $d=15.8$ mm, and length $l=200$ mm) which were attached both to the entrance and the exit sides of a rectangular resonator (height $H=7.8$ mm, width $D=39$ mm, and length $L=176$ mm). At the junctions to the cavity metallic diaphragms of different openings were inserted (Fig. 1). The microwaves with frequencies between 12.3 and 18.0 GHz, where two even transverse modes are excited in the cavity and one transverse mode in each of the leads, are coupled into the waveguide via an adaptor to ensure strong coupling.

The experimental results are compared with the predictions of the MRGM. We solve the S matrix for the single-particle Schrödinger equation for this "quantum dot" by assuming a constant potential set equal to zero inside and
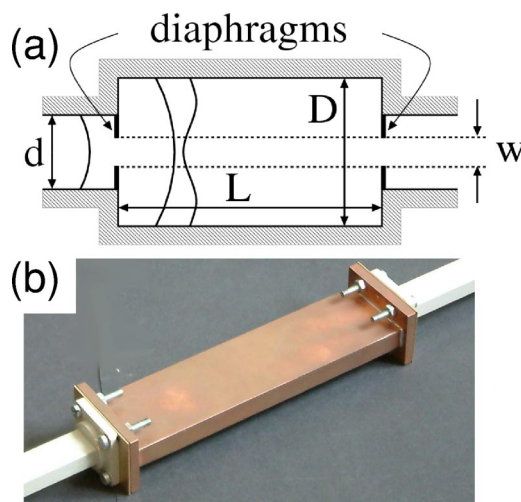
FIG. 1. (Color online) (a) Schematic sketch of the rectangular cavity with leads attached symmetrically on opposite sides. Exchangeable diaphragms at the lead junctions allows one to control the coupling between the cavity and the leads. The open even transverse states are indicated. (b) Photograph of the experimental setup.

*Electronic address: rotter@concord.itp.tuwien.ac.at

infinitely high outside a hard-wall boundary. At asymptotic distances, scattering boundary conditions are imposed on the leads. The coupling of the leads to the cavity of length L can be varied by two diaphragms which are placed symmetrically at the two lead openings. The lead width d and the width of the rectangular cavity D determine how many flux-carrying modes are open at a certain energy ε in each of the three regions (lead-cavity-lead). We consider in the following the range of wave numbers where one flux-carrying mode is open in each of the leads, while the first and second even transverse modes are open inside the cavity, thus providing two alternative pathways of quantum transport. In order to further characterize the interfering paths, we decompose the transport across the cavity into a multiple-scattering series involving three pieces [20], each of which is characterized by a mode-to-mode transmission (reflection) amplitude or a propagator: (1) the transmission of the incoming flux from the left into the cavity, $t^{(L)}$, or reflection back into the lead, $r^{(L)}$, (2) the propagation inside the cavity from the left to the right, $G^{(LR)}$, or from the right to the left, $G^{(RL)}$, and (3) the transmission from the interior of the cavity to the right, $t^{(R)}$, or internal reflection at each of the two vertical cavity walls with amplitude $r^{(R)}$. For the Green's functions (i.e., propagators) $G^{(LR)}(x_R,x_L)$ and $G^{(RL)}(x_L,x_R)$ we choose a mixed representation which is local in x, and employs a spectral sum over transverse modes, $G^{(LR)}(x_R,x_L) = G^{(RL)}(x_L,x_R) = \Sigma_n |n\rangle \exp(ik_n|x_R-x_L|)\langle n|$, where $x_{R,L}$ are the x coordinates of the right (left) lead junction with $|x_R-x_L|=L$. The longitudinal momentum for each channel n in the cavity is given by $k_n = \sqrt{k^2-(k_n^c)^2}$, with the momentum $k=\sqrt{2\varepsilon}$ and the threshold k values $k_n^c=n\pi/D$. Decoherence due to dissipation of the microwave power in the cavity walls can be easily incorporated by analytically continuing k_n into the complex plane, $k_n = \sqrt{k^2-(k_n^c)^2}+i\kappa$. The quantitative analysis of Fano resonances for these systems can be used to accurately determine the degree of dissipation present. The multiple-scattering expansion of the transmission amplitude T is then given by

$$T(k) = t^{(L)}G^{(LR)}\left\{ \sum_{n=0}^{\infty} [r^{(R)}G^{(RL)}r^{(L)}G^{(LR)}]^n \right\} t^{(R)}$$
$$= t^{(L)}G^{(LR)}[1 - r^{(R)}G^{(RL)}r^{(L)}G^{(LR)}]^{-1}t^{(R)}. \qquad (1)$$

The identification of the resonant and nonresonant pathways with help of Eq. (1) is straightforward: due to the absence of interchannel mixing in the rectangular (i.e., nonchaotic) cavity, the nonresonant contribution corresponds to the $n=0$ term of the sum describing direct transmission while the resonant contribution is made up by all multiple-bounce contributions ($n \geq 1$). The various amplitudes entering Eq. (1) can be parametrized in terms of four phases and two moduli [21]: the modulus s of the reflection amplitude of the wave incoming in mode 1 and reflected into mode 1 at the left diaphragm,

$$r_{11}^{(L)} = se^{i\phi_r}, \qquad (2)$$

and the modulus p of the partial injection amplitude of the incoming wave into the lowest mode of the cavity, corrected for the partially reflected flux,

$$t_{11}^{(L)} = t_{11}^{(R)} = p\sqrt{1-s^2}e^{i\phi_t^{(1)}}. \qquad (3)$$

Because of the symmetry of the scattering device, the injection (ejection) amplitude at the left (right) side are equal. Accordingly, the injection amplitude into the second even mode of the cavity is given by

$$t_{12}^{(L)} = t_{21}^{(R)} = \sqrt{(1-p^2)(1-s^2)}e^{i\phi_t^{(2)}}. \qquad (4)$$

Analogous expressions can be deduced [21] for the other partial amplitudes entering Eq. (1). We omit a detailed description of the phases in Eqs. (2)–(4) since they do not explicitly enter our analysis in the following. The key observation in the present context is that the square module s^2 is monotonically decreasing in between the limiting values $s^2 =1$ for zero diaphragm opening ($w=0$) and $s^2 \approx 0$ for fully open diaphragms ($w=d$). Inserting Eqs. (2)–(4) into Eq. (1), a closed yet complicated expression for the transmission probability $|T(\varepsilon,s)|$ as a function of the energy ε and the opening parameter s can be derived. Close to a given resonance ε_i^R this expression can be approximated by the Fano form [3,21]

$$|T(\varepsilon,s)|^2 \approx \frac{|\varepsilon - \varepsilon_i^R(s) + q_i(s)\Gamma_i(s)/2|^2}{[\varepsilon - \varepsilon_i^R(s)]^2 + [\Gamma_i(s)/2]^2}, \qquad (5)$$

where $\varepsilon_i^R(s)$ is the position of the ith resonance, $\Gamma_i(s)$ its width, and $q_i(s)$ the complex Fano asymmetry parameter, all of which depend on s. Window resonances appear in the limit $q \to 0$ while the Breit-Wigner limit is reached for $|q| \gg 1$. It should be noted that, in general, q cannot be simply identified with the ratio of resonant to nonresonant coupling strength [22,23]. Moreover, since Fano resonances can be identified as resulting from the interference between resonances related to the eigenmodes in the cavity, the parameter q depends very sensitively on the specific constellation of the involved resonance poles [24,25]. Figure 2 presents both the experimental and theoretical dependence of the transmission probability $|T|^2$ on k (or ε). In the measurement, the diaphragms were successively closed in steps of 1 mm. The data sets of Figs. 2(a)–2(c) represent the transmission probability for three different values of the opening of the diaphragms $w=5.8$, 8.8, and 15.8 mm, respectively. Note the remarkable degree of agreement between the measured and the calculated data without any adjustable parameter. In Fig. 2(a) where $w/d \approx 0.37$, transport is suppressed and mediated only by resonance scattering with narrow Breit-Wigner shapes centered at the eigenenergies of the closed billiard as indicated by the tick marks. With increasing diaphragm opening [Fig. 2(b)] transport acquires a significant nonresonant contribution, leading to the widening and the overlap of resonances. Finally, for fully open leads [Fig. 2(c)], $w/d=1$ (or $s \approx 0$) resonances appear as narrow window resonances in a nonresonant continuum. The trajectory of the resonance parameter as a function of s can be both experimentally and theoretically mapped out in considerable detail.

Different types of resonances can be identified by characteristically different variations of their resonance parameters. The evolution of the Fano parameter as a function of w/d (or
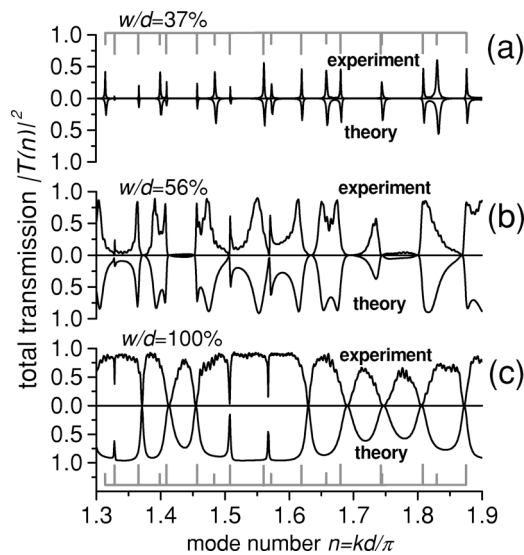
FIG. 2. Total transmission probability $T^{\text{tot}}(\sqrt{2\varepsilon}d/\pi, w/d)$ for transport through the rectangular cavity with three different openings of the diaphragms: (a) $w/d=37\%$, (b) $w/d=56\%$, and (c) $w/d=100\%$. For better comparison, the experimental and the calculated results are shown as mirror images. The positions of all eigenstates in the closed cavity are indicated by the gray tick marks. For all the calculated curves shown, a damping constant of $\kappa=10^{-4}$ was used.

s) for one resonance is highlighted in Fig. 3. The transition from a narrow Breit-Wigner resonance via a somewhat wider asymmetric Fano profile to a window resonance is clearly observable. The good agreement with theory allows one to accurately determine the degree of decoherence present in the experiment. As the Fano profile, in particular, near its
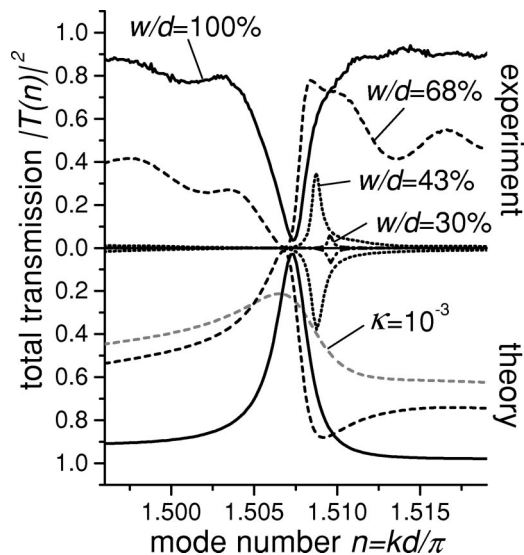
FIG. 3. Fano resonance near the second even excited transverse mode at $kd/\pi \approx 1.5095$. Experimental and theoretical results for four different cavity openings (w/d) are shown. Curves with equal w/d ratio are displayed in the same line style (solid, dashed, dotted, and dash-dotted). For all calculated curves a damping factor $\kappa=10^{-4}$ was used, except for the additional gray dashed curve shown for which $\kappa=10^{-3}$ and $w/d=0.68$.
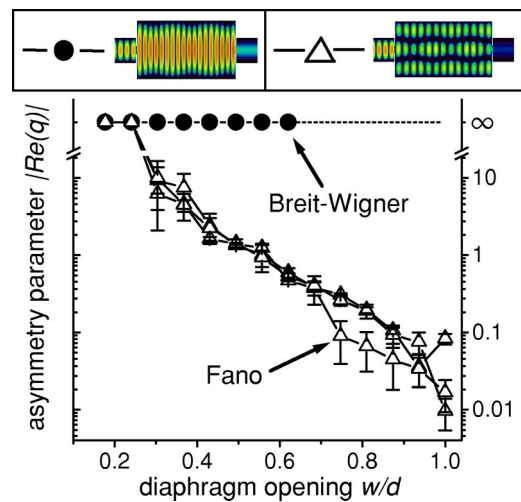
FIG. 4. (Color online) Real part of the asymmetry parameter $|\text{Re}(q)|$ as a function of the diaphragm opening w/d. The data represent fits to the experiment. Solid circles • (open triangles △) correspond to resonances originating from the first (second) even cavity eigenstate. Typical wave functions $|\psi(x,y)|^2$ for these two classes of resonances are shown in the inset. The • resonances always keep an $|\text{Re}(q)| > 10$, above which the Fano resonances are very close to the Breit-Wigner line shape $[\text{Re}(q)=\infty]$. The △ resonances undergo a complete evolution from Breit-Wigner to window type as w/d varies between 0 and 1.

minimum, is very sensitive to any noninterfering incoherent background, we can determine an upper bound for the damping by comparison between experiment and theory to be $\kappa \lesssim 10^{-4}$. As illustrated in Fig. 3, even a slightly larger value of $\kappa=10^{-3}$ would drastically deteriorate the agreement between experiment and theory. In line with the value $\kappa=10^{-4}$, we obtain an imaginary part of the complex Fano parameter for systems without time-reversal symmetry [19] out of our fitting procedure as $\text{Im } q \lesssim 0.1$. We note that by using superconducting cavities κ could still be further reduced [26], however with only limited influence on the result, since we have already nearly reached the fully coherent limit.

Following the parametric evolution of a large number of resonances we find a characteristic pattern of Fano resonance parameters (Fig. 4). As example we show the evolution of the q parameter as a function of the opening w/d. Obviously, two distinct subsets of resonances appear in the rectangular billiards: one set is characterized by a large and only weakly dependent asymmetry parameter q. A second set of resonances features a strongly varying q (on the log-scale) from large values near the Breit-Wigner limit to values close to $q \approx 0$ for wide opening, yielding a window resonance. For these resonances, the width Γ first increases with w/d increasing from close to 0, then reaches a local maximum, and finally decreases slightly when $w/d \to 1$ (not shown). A similar nonmonotonic behavior of Γ was recently observed in a single-electron transistor experiment [9]. Such features can be understood in terms of avoided crossings in the complex plane [13,14] between interacting resonances. While the von Neumann–Wigner theorem [27] for bound states predicts avoided crossings between states of the same symmetry and

thus a nonmonotonic variation of the eigenenergy, interacting resonances can also display avoided crossings on the imaginary axis, i.e., exchange of the width of resonances and thus leading to a nonmonotonic behavior of one of the Γ's involved. The two resonance poles approach each other in the complex energy plane and undergo an avoided crossing as a function of the coupling parameter s. As a result of this "resonance trapping" effect, the larger resonance gets even larger for increasing s and will form a background, on top of which an increasingly narrow resonance is situated [15].

For the present system, the interacting resonances can be completely characterized in terms of scattering wave functions that can be unambiguously determined theoretically (see inset Fig. 4). Resonances that undergo a complete evolution from Breit-Wigner resonances to a window resonance are all associated with the second even excited state in the cavity, while resonances that maintain their Breit-Wigner shape are connected to transport through the transverse ground state of the cavity. This mapping is controlled by the amplitude p for transmission through the first transverse mode [see Eqs. (3) and (4)]. In the case that $p^2 > 1/2$ all resonances associated with the first mode are broader than the resonances associated with the excited state and vice versa for $p^2 < 1/2$. For geometric reasons the scattering device studied here (Fig. 1) always favors transport through the first cavity mode and therefore $p^2 > 1/2$. In this way we arrive at the remarkably simple result that all resonances associated with a first mode feature a weakly varying q, while all resonances associated with the second mode undergo the complete evolution from the Breit-Wigner to the window

limit. This one-to-one mapping is supported by the data of Fig. 2, where only second-mode resonances (indicated by the long tick marks) "survive" the transition of $w/d \to 1$, while all first-mode resonances (short tick marks) vanish in the background of the transmission spectrum. The present observation has far-reaching implications for other systems. By tracing the evolution of a given resonance as a function of a control parameter the nature of the resonant channel can be uniquely determined.

In summary, the rectangular microwave cavity attached to two leads allows one to study the interplay between resonant and nonresonant transport in unprecedented detail. By controlled change of the opening, tuning a Fano resonance from the Breit-Wigner limit to the window resonance limit has become possible. Fano resonances can be used to accurately determine the degree of decoherence present in a scattering device. Nonmonotonic behavior of resonance parameters can be related to avoided crossings between interacting resonances, which can be unambiguously associated with different resonant modes of the cavity. The latter feature is a consequence of the separability of the wave function in the closed cavity. Future investigations along these lines for nonseparable chaotic cavities promise new insights into the resonance dynamics of open chaotic systems.

[1] H. Beutler, Z. Phys. **93**, 177 (1935).

[2] U. Fano, Nuovo Cimento **12**, 156 (1935).

[3] U. Fano, Phys. Rev. **124**, 1866 (1961).

[4] R. Adair, C. Bockelman, and R. E. Peterson, Phys. Rev. **76**, 308 (1949).

[5] J. Simpson and U. Fano, Phys. Rev. Lett. **11**, 158 (1963).

[6] F. Cerdeira, T. Fjeldly, and M. Carpona, Phys. Rev. B **8**, 4734 (1973).

[7] J. Feist, F. Capasso, C. Sirtori, K. West, and L. Pfeiffer, Nature (London) **390**, 589 (1997).

[8] V. Madhavan, W. Chen, T. Jamneala, M. Crommie, and S. Wingreen, Science **280**, 567 (1998).

[9] J. Göres, Phys. Rev. B **62**, 2188 (2000).

[10] J. U. Nöckel and A. D. Stone, Phys. Rev. B **50**, 17415 (1994).

[11] S. Rotter *et al.*, Phys. Rev. B **68**, 165302 (2003).

[12] K. Kobayashi *et al.*, Phys. Rev. Lett. **88**, 256806 (2002).

[13] W. D. Heiss and A. L. Sannino, J. Phys. A **23**, 1167 (1990); Phys. Rev. A **43**, 4159 (1991).

[14] J. Burgdörfer, X. Yang, and J. Müller, Chaos, Solitons Fractals **5**, 1235 (1995).

[15] J. Okołowicz, M. Płoszajczak, and I. Rotter, Phys. Rep. **374**, 271 (2003), and references therein.

[16] E. Persson, I. Rotter, H.-J. Stöckmann, and M. Barth, Phys. Rev. Lett. **85**, 2478 (2000).

[17] H. J. Stöckmann, *Quantum Chaos: An Introduction* (Cambridge University Press, Cambridge, 1999).

[18] S. Rotter *et al.*, Phys. Rev. B **62**, 1950 (2000).

[19] A. A. Clerk, X. Waintal, and P. W. Brouwer, Phys. Rev. Lett. **86**, 4636 (2001).

[20] L. Wirtz, C. Stampfer, S. Rotter, and J. Burgdörfer, Phys. Rev. E **67**, 016206 (2003).

[21] D.-H. Kim, H.-S. Sim, and K. J. Chang, Phys. Rev. B **64**, 115409 (2001); **67**, 129903(E) (2003).

[22] U. Eichmann, T. F. Gallagher, and R. Konik, Phys. Rev. Lett. **90**, 233004 (2003).

[23] H. Friedrich, *Theoretical Atomic Physics* (Springer, Berlin, 1998), Chap. 3.

[24] H.-W. Lee, Phys. Rev. Lett. **82**, 2358 (1999).

[25] A. I. Magunov, I. Rotter, and S. I. Strakhova, Phys. Rev. B **68**, 245305 (2003).

[26] A. Richter, in *Emerging Applications of Number Theory*, edited by D. A. Hejhal *et al.*, Mathematics and its Applications Vol. 109 (Springer, New York, 1999), p. 479.

[27] J. von Neumann and E. Wigner, Phys. Z. **30**, 467 (1929).